Supplementary material for

Synthesis, crystal structure, and properties of stoichiometric hard tungsten tetraboride, WB_4

Elena Bykova,[1,2] Sergey V. Ovsyannikov,[1] Maxim Bykov, [3] Yuqing Yin,[4,5] Timofey Fedotenko[6], Hendrik Holz,[7] Stefan Gabel,[7] Benoit Merle,[7] Stella Chariton,[8] Vitali B. Prakapenka,[8] Natalia Dubrovinskaia,[4,9] Alexander F. Goncharov[2], and Leonid Dubrovinsky[1]

[1] Bayerisches Geoinstitut, University of Bayreuth, Universitätsstrasse 30, D-95447, Bayreuth, Germany

[2] Earth and Planets Laboratory, Carnegie Institution for Science, 5241 Broad Branch Road, NW, Washington DC, 20015, USA

[3] Institute of Inorganic Chemistry, University of Cologne, Greinstrasse 6, 50939 Cologne, Germany

[4] Material Physics and Technology at Extreme Conditions, Laboratory of Crystallography, University of Bayreuth, 95440 Bayreuth, Germany

[5] State Key Laboratory of Crystal Materials, Shandong University, Jinan 250100, China

[6] Photon Science, Deutsches Elektronen-Synchrotron, Notkestrasse 85, 22607 Hamburg, Germany

[7] Friedrich-Alexander-Universität Erlangen-Nürnberg, Department of Materials Science and Engineering, Institute I, Interdisciplinary Center for Nanostructured Films (IZNF), Cauerstr. 3, 91058 Erlangen, Germany

[8] Center for Advanced Radiation Sources, The University of Chicago, 5640 S. Ellis, Chicago, IL, 60637, USA

[9] Department of Physics, Chemistry and Biology (IFM), Linköping University, SE-58183 Linköping, Sweden

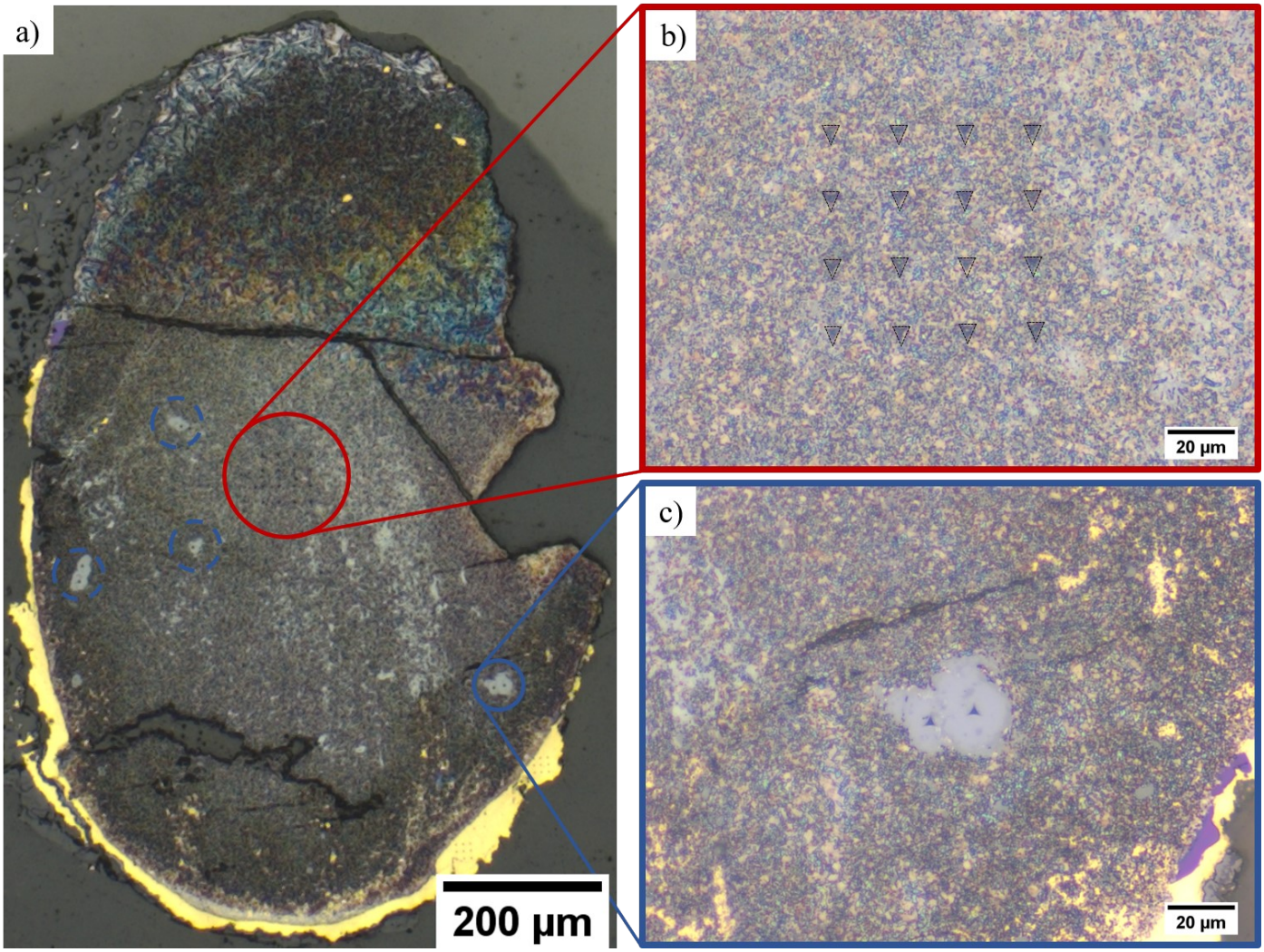

Figure S1. Optical micrographs of the sample after nanoindentation. Overview (*a*) with the areas of interest shown as insets. The red rectangle magnifies a likely polycrystalline region; black triangles that mark the position of the indents (*b*). The blue rectangle magnifies a likely single crystalline region (*c*).

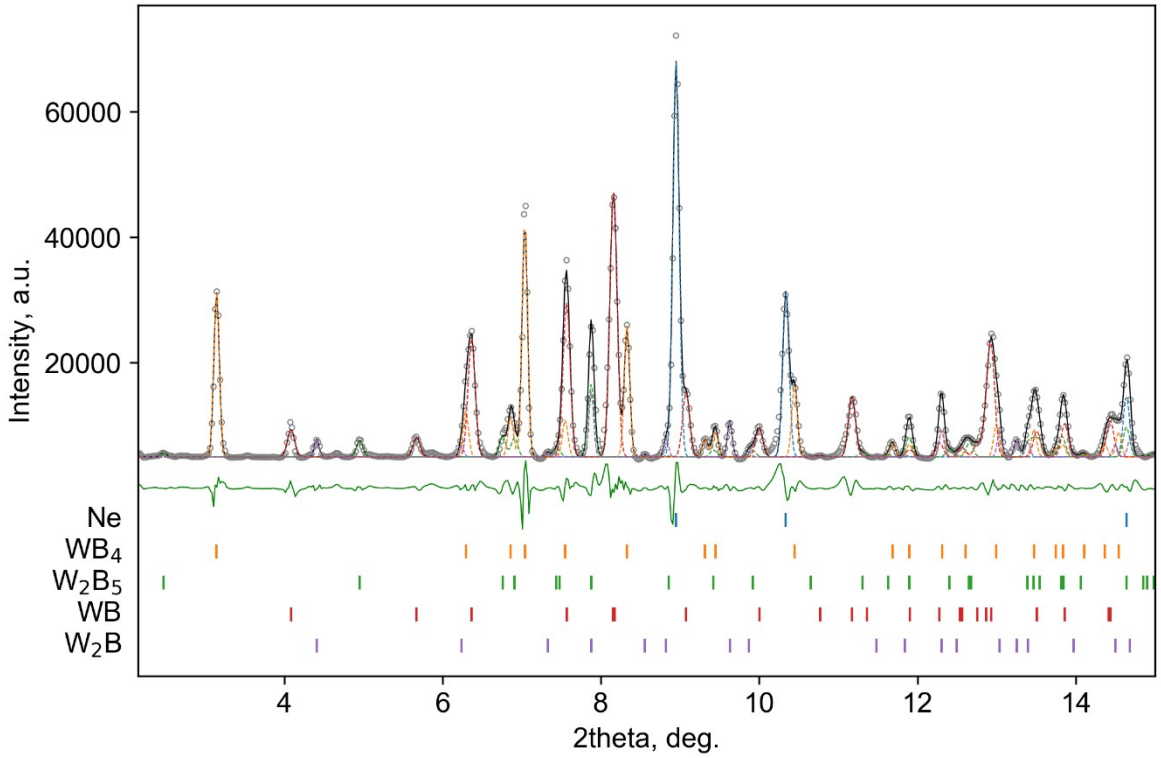

Figure S2. Powder X-ray diffraction pattern collected at 30.3(5) GPa after the laser heating up to 2300(100) K (λ = 0.2952 Å): the experimental data are shown by grey circles (the background was subtracted), a Le Bail fit – by dash lines (WB_4 – orange, W_2B_5 – green, WB – red, W_2B – violet, Ne pressure medium - blue), a difference curve –by the green solid line; the ticks show predicted positions of the diffraction peaks.

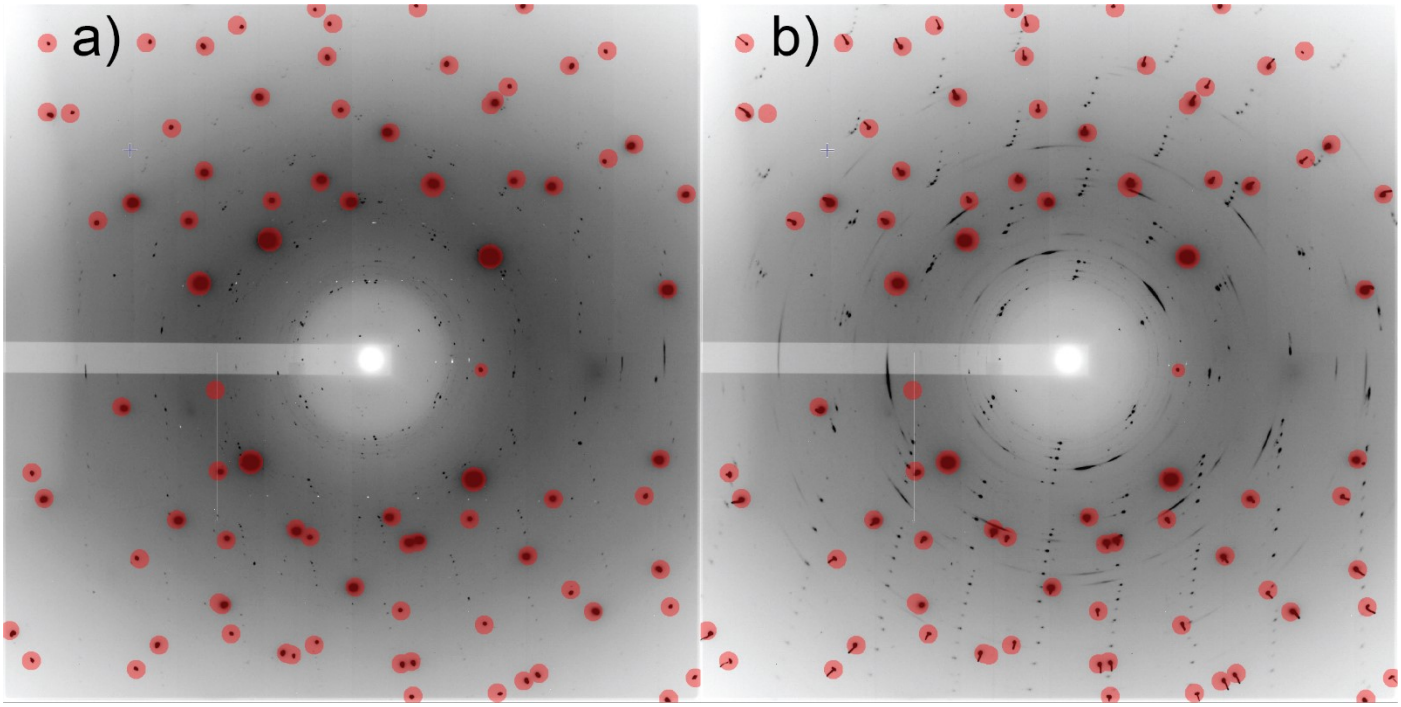

Figure S3. X-ray diffraction wide images of WB_4 single crystal in a diamond anvil cell at 2.8(5) (*a*) and 53.2(5) GPa (*b*). The difference in the peaks intensity is attributed to a fact that at each pressure point the data collection was done at a slightly different spot on the crystal since the crystal's size (10 x 10 x 5 μm^3) was larger than the X-ray beam (focal spot ~3 μm). Large masked intense spots are diffraction peaks from diamond, elongated peaks belong to Ne pressure medium.

Table S1. Experimental conditions in laser heating experiments in DAC and in multi-anvil apparatus.

Initial phase composition	**Pressure, GPa**	**Maximal temperature, K**	**Final phase composition**
Laser-heating experiments in DAC			
Amorphous boron, W foil	17.1(5)	2850(200)	W_2B, WB, W_2B_5
Amorphous boron, W foil	30.3(5)	2300(100)	W_2B, WB, W_2B_5, WB_4

Multi-anvil experiments				
Initial phase composition	**Pressure range, GPa**	**Temperature, K**	**Heating duration, hours**	**Final phase composition**
Amorphous boron + W foil	20	2073	2	WB_4, WB_2
Amorphous boron + W powder	23	2273	3	WB_4 polycrystal
Amorphous boron + W	20	2073	36	WB_2, WB_4 crystals

Table S2. Details of crystal structure refinements for WB_4 at high pressures (sp.gr. *P6₃/mmc*; *Z* = 2; W1 2*d* (2/3, 1/3, 1/4), B1 4*f* (1/3, 2/3, *z*), B2 4*f* (1/3, 2/3, *z*))

Pressure, GPa	0.0001	2.80(2)	5.9(5)	8.6(5)	12.0(5)	16.5(5)	21.4(5)	25.9(5)	31.2(5)	36.5(5)	42.2(5)	47.9(5)	53.2(5)
***a* (Å)**	2.9578(6)	2.9349(4)	2.9240(3)	2.9185(6)	2.9014(3)	2.8905(3)	2.8726(2)	2.8625(3)	2.8438(3)	2.8307(4)	2.8240(4)	2.8068(4)	2.7932(5)
***c* (Å)**	10.996(3)	10.902(18)	10.861(4)	10.821(19)	10.821(6)	10.793(4)	10.730(3)	10.713(5)	10.664(6)	10.619(6)	10.589(10)	10.567(5)	10.528(9)
***V* (Å^3)**	83.31(4)	81.32(14)	80.42(3)	79.82(14)	78.89(5)	78.10(4)	76.68(2)	76.02(4)	74.69(5)	73.69(5)	73.13(7)	72.09(4)	71.14(7)
ρ_{calc} (g/cm^3)	9.053	9.274	9.379	9.448	9.56	9.657	9.835	9.921	10.097	10.235	10.313	10.461	10.602
μ/mm^{-1}	36.86	6.687	6.762	6.812	6.893	6.963	7.092	7.153	7.28	7.379	7.436	7.543	7.644
$2\Theta_{min}$ for data collection (°)	5.855	3.27	3.283	3.289	3.308	3.321	3.341	3.442	3.464	3.48	3.489	3.42	3.436
$2\Theta_{max}$ for data collection (°)	23.454	18.006	17.5	16.812	17.623	13.974	15.246	13.737	15.208	15.28	15.17	16.843	15.232
Completeness to *d* = 0.8 Å	0.98	0.54	0.571	0.388	0.673	0.592	0.583	0.562	0.596	0.617	0.565	0.587	0.6
Reflections collected	331	394	222	181	353	261	242	276	288	289	253	245	214
Independent reflections	69	79	82	57	98	62	73	56	71	72	70	87	67
Independent reflections [$I > 2\sigma(I)$]	66	69	73	50	87	56	67	51	66	67	64	79	62
Refined parameters	7	7	7	7	7	7	7	7	7	7	7	7	7
$R_{int}(F^2)$	0.0322	0.044	0.0249	0.0451	0.0412	0.0455	0.0543	0.0619	0.0293	0.0282	0.0444	0.0192	0.0206
$R(\sigma)$	0.019	0.0374	0.0309	0.0404	0.0315	0.0315	0.0326	0.045	0.0225	0.0207	0.0508	0.0171	0.0148
R_1 [$I > 2\sigma(I)$]	0.0212	0.0243	0.0212	0.0368	0.0244	0.0251	0.0281	0.037	0.0233	0.0217	0.0216	0.0223	0.0217
wR_2 [$I > 2\sigma(I)$]	0.0449	0.055	0.0493	0.0829	0.058	0.0599	0.067	0.0697	0.05	0.0504	0.0513	0.0512	0.0542
R_1	0.0264	0.0321	0.0226	0.0412	0.0271	0.0254	0.0309	0.0383	0.0243	0.023	0.0248	0.0234	0.0223
wR_2	0.0459	0.0572	0.0502	0.0849	0.0594	0.0601	0.0694	0.071	0.0506	0.0511	0.0522	0.0518	0.0545
Goodness of fit on F^2	1.244	1.06	1.122	1.156	1.17	1.105	1.356	1.129	1.191	1.181	1.139	1.242	1.281
$\Delta\rho_{max}$(*e* / Å^3)	2.088	2.449	2.529	2.108	1.557	1.82	2.5	2.584	2.235	2.04	2.087	2.192	2.271
$\Delta\rho_{min}$(*e* / Å^3)	-1.599	-2.228	-1.562	-2.4	-2.411	-2.259	-2.448	-2.604	-1.822	-1.83	-1.687	-1.752	-2.116
***z*(B1)**	0.5466(13)	0.546(3)	0.5422(16)	0.541(7)	0.546(2)	0.547(3)	0.545(3)	0.550(4)	0.546(2)	0.5457(19)	0.550(3)	0.5469(16)	0.546(2)
***z*(B2)**	0.1106(13)	0.116(3)	0.1115(19)	0.114(7)	0.112(2)	0.111(3)	0.115(3)	0.111(4)	0.113(2)	0.113(2)	0.112(3)	0.1114(18)	0.113(2)
U_{eq}(Re1) (Å^2)*	0.0030(3)	0.0081(5)	0.0052(2)	0.0070(9)	0.0063(2)	0.0049(4)	0.0038(3)	0.0062(6)	0.0061(3)	0.0059(3)	0.0070(3)	0.0055(2)	0.0064(3)
U_{iso}(B1) (Å^2)	0.002(2)	0.0064(18)	0.0023(15)	0.008(4)	0.0079(18)	0.005(3)	0.004(2)	0.008(4)	0.0054(18)	0.0031(16)	0.004(2)	0.0038(13)	0.0052(18)
U_{iso}(B2) (Å^2)	0.003(3)	0.0059(17)	0.0062(18)	0.008(4)	0.0061(16)	0.003(2)	0.006(2)	0.007(4)	0.0047(17)	0.0059(18)	0.006(2)	0.0056(14)	0.0060(19)
***d1*(W1...B2) (Å)**	2.237(15)	2.24(2)	2.261(14)	2.24(5)	2.244(14)	2.244(19)	2.20(2)	2.22(3)	2.195(15)	2.189(16)	2.19(2)	2.184(13)	2.163(16)
***d2*(W1...B1) (Å)**	2.295(10)	2.22(3)	2.257(18)	2.26(7)	2.21(2)	2.19(3)	2.20(3)	2.15(5)	2.17(2)	2.17(2)	2.11(3)	2.146(17)	2.15(2)
***d3*(B1−B2) #1 (Å)**	1.73(2)	1.77(5)	1.67(3)	1.68(11)	1.71(3)	1.71(4)	1.71(4)	1.73(7)	1.70(3)	1.68(3)	1.72(4)	1.67(3)	1.67(3)
***d4*(B1−B2) #2 (Å)**	1.847(7)	1.854(18)	1.848(11)	1.86(4)	1.822(13)	1.805(17)	1.822(18)	1.78(2)	1.792(13)	1.784(12)	1.758(15)	1.758(10)	1.762(13)
***d5*(B1−B1) (Å)**	1.991(15)	1.97(3)	1.921(17)	1.91(7)	1.95(2)	1.96(3)	1.92(3)	1.97(5)	1.91(2)	1.90(2)	1.95(3)	1.900(18)	1.88(2)
Data collection	In house	DESY, Extreme Conditions Beamline, Perkin Elmer detector, λ = 0.2900 Å											
CSD number	2158536	2158520	2158521	2158522	2158523	2158524	2158525	2158526	2158527	2158528	2158529	2158530	2158531

*U_{eq} is defined as one third of the trace of the orthogonalized U^{ij} tensor.